
CHAPTER 7**EFFECT OF CONDITIONING pH ON SULPHUR, GOLD AND URANIUM FLOTATION**

7.1 Introduction

The feed treated at No 2 Gold Plant consists of a mixture of tailings from the cyanidation of run-of-mine ore and reclaimed dump material. Exposure of this feed to air and water, coupled with the use of air during leaching all subject the sulphide minerals to surface oxidation. Oxidized surfaces inhibit their reaction with collector molecules. For optimal recovery, the negative effect of surface oxidation has to be overcome.

Examination of thermodynamic data for metal-water systems shows certain E_h -pH conditions in which metals are more stable in their cationic form (Jackson, 1986). Subjecting oxides to these conditions promotes their dissolution in order to achieve the thermodynamically supported species. In this view, treatment of the oxidised flotation feed at low pH in the presence of dissolved oxygen should favour the removal of iron oxides formed on pyrite, thereby exposing underlying fresh sulphide. This is likely to improve interaction with SIBX, and hence flotation response.

Based on this background, the effect of a low pH treatment prior to flotation was investigated on No. 2 Gold Plant feed. After the initial conditioning for 1 minute, 1.25kg/t of sulphuric acid was added and the pH decreased from 7.8 to 1.9. At the same time, the pulp potential increased from 0.3V to 0.6V^Ω. The pulp was conditioned for 10 minutes, the pH rose to 3.7 and the potential decreased to 0.5V. A caustic solution was added to achieve the standard

^Ω All pulp potentials are reported versus the standard hydrogen electrode

flotation pH of 7.2. At this point, the pulp potential was 0.3V. Flotation was then carried out using the reagent suite of the standard.

7.2 Results and Discussion

7.2.1 Sulphur

Table 7.1 shows sulphur flotation initial rates and corresponding final recoveries for the two conditioning pHs. The initial rate of 0.91min^{-1} at pH 1.9^φ indicates significantly higher sulphur flotation kinetics compared to the 0.66min^{-1} recorded at pH 7.2. This shows that conditioning at this low pH activated sulphide surfaces, which improved interaction with flotation reagents.

Table 7.1 *Sulphur final recoveries and initial rates*

Conditioning pH	k (min ⁻¹)	R _{max} (%)	R ²
1.9	0.91	72.5	0.9995
7.2	0.66	77.4	0.9987

Table 7.2 shows pulp potential and pH values recorded during conditioning. Superimposing these data on the Pourbaix diagram of the Fe-S-H₂O system can give an indication of the thermodynamically stable species, and hence reactions that took place during conditioning.

Table 7.2 *Pulp pH and potentials recorded during conditioning*

	Natural E _h -pH	After acid dosage	After 10 min conditioning	After caustic dosage	During Flotation
pH	7.8	1.9	3.7	7.2	7.2
Potential (V)	0.3	0.6	0.5	0.3	0.04

^φ This will be referred to as “pH 1.9 conditioning” throughout this discussion even though pH rose throughout conditioning until it stabilised at 3.7

Figure 7.1 shows that the natural pulp pH and potential recorded for the flotation feed (point A) coincide with the domain in which ferric oxide⁸ is thermodynamically stable. Immediately after sulphuric acid was added, the two responses shifted to point B, which lies in the domain of ferrous ion stability.

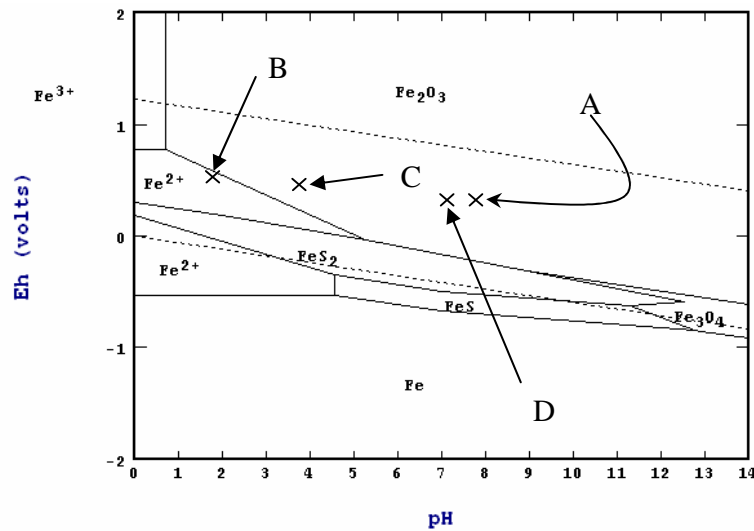


Figure 7.1 A Pourbaix diagram for the Fe-S-H₂O system at 25°C, 10⁻⁴M [Fe], 10⁻⁴M [S] showing E_h-pH conditions prevailing during conditioning [A] natural pulp E_h-pH, [B] after addition of 1.25kg/t sulphuric acid, [C] after 10 minutes of conditioning, [D] after dosage of a caustic solution to attain standard flotation pH

Any superficial iron oxide on pyrite particles should leach to form ferrous ions. This exposes the underlying sulphide, so that it can interact freely with flotation reagents. This probably accounts for the higher flotation kinetics.

Figure 7.2 shows sulphur recovery-grade curves plotted for the two conditioning pHs. Even though pH 1.9 seemed superior at the beginning of the experiment, the difference was small. By the end of both flotation experiments, pH 7.5 had recorded a higher final recovery (Table 7.1). Figure 7.1 shows that after addition of caustic, the new pulp pH and potential fell in the domain of ferric oxide (point C). If solubility limits were exceeded, then ferric hydroxide should have precipitated. Because precipitation is not

⁸ Under normal conditions, the hydrated form of this oxide is formed

selective between sulphide and gangue, the hydroxide could have formed on pyrite, which is likely to depress it. For the iron ions that remained in solution, they can form a number of hydroxyl complexes with caustic. These are likely to affect pyrite flotation with xanthate.

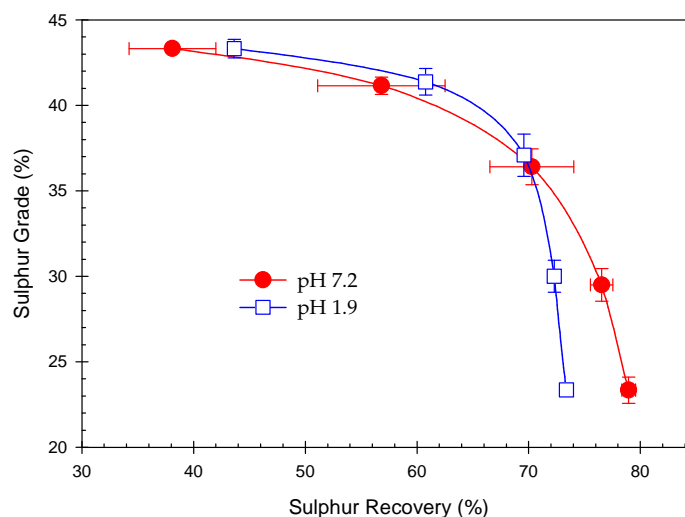


Figure 7.2 Sulphur recovery-grade curves

Jiang and co-workers (1998) observed significant depression in the neutral pH range after $2 \times 10^{-3}\text{M}$ Fe^{3+} ions were added to ore pyrite at pH 3, which was followed by adjustment of pulp pH to flotation pH and dosage of $3.3 \times 10^{-4}\text{M}$ ethyl xanthate and 50mg l^{-1} MIBC. A similar exercise using ferrous ions showed more significant depression in the same pH range. Examination of speciation diagrams in Figures 7.3 and 7.4 plotted using STABCAL software for the concentration of ferrous and ferric ions tested by Jiang et al. (1998) predicts Fe^{2+} , FeOH^+ and $\text{Fe}(\text{OH})_3$ to be the stable species in the neutral pH range.

By using iron-xanthate-water system distribution diagrams, the authors showed that in neutral to weakly alkaline conditions (pH 5-9.5), some hydroxyl xanthate species are formed, namely $(\text{Fe}(\text{OH})\text{X})_2$ and $\text{Fe}(\text{OH})\text{X}$. Since FTIR measurements by Wang (1995) suggested that ferric xanthate is

adsorbed on pyrite, Jiang and co-workers (1998) attributed the lower recoveries to the lower hydrophobicity exhibited by the two complexes.

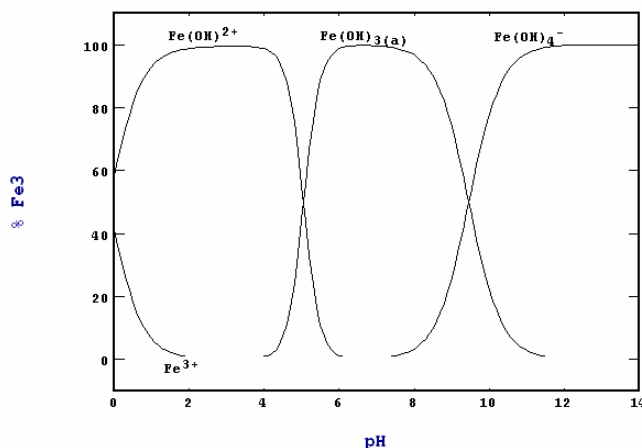


Figure 7.3 Speciation diagram for $2 \times 10^{-3}M$ Fe(III) as a function of pH at 25°C. STABCAL Software, NBS Database

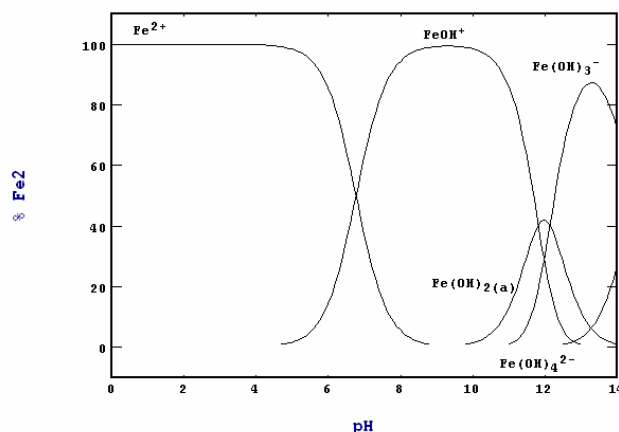


Figure 7.4 Speciation diagram for $2 \times 10^{-3}M$ Fe(II) as a function of pH at 25°C. STABCAL Software, NBS Database

The depression of pyrite flotation following conditioning at pH 1.9 is probably due to the two hydroxyl-xanthate species. The above speciation diagrams suggest that conditioning at pH 1.9 promotes the formation of $Fe(OH)^{2+}$, Fe^{2+} and $Fe(OH)^+$ in the pulp. When pH is raised to 7.2 using a caustic solution, only $Fe(OH)_3$ is the stable iron (III) species formed. Iron (II)

forms FeOH^+ and Fe^{2+} only. Addition of xanthate results in the formation of $(\text{Fe}(\text{OH})\text{X})_2$ and $\text{Fe}(\text{OH})^+\text{X}$ and ferrous xanthate as well. Due to its high solubility, ferrous xanthate is unlikely to precipitate. For enhancement of pyrite flotation, all these complexes have to either form on the surface or adsorb after formation in solution (Davidtz, 2005). Failure to interact with the surface will give poor flotation response since there will be less xanthate available to impart hydrophobicity to pyrite. Since it is not always possible that all the ferrous hydroxyl xanthates formed in solution will adsorb onto pyrite, the presence of ferrous ions might have contributed to the lower sulphide final recoveries in Figure 7.2.

Jiang et al. (1998) have showed that at a modest degree of oxidation; pyrite surfaces behave like iron oxide with a PZC at pH 7. This is due to the presence of ferric hydroxide formed during oxidation. The surface will acquire electrokinetic features of the iron hydroxide. The authors showed that in the presence of $2 \times 10^{-3}\text{M}$ ferric ions and $6.6 \times 10^{-4}\text{M}$ ethyl xanthate, the zeta potential of pyrite exhibited less positive charge below pH 7.5 compared with that in the presence of ferric xanthate alone. At $\text{pH} > 7.5$, there was no noticeable difference between the two. This implies that in the presence of ferric ions, adsorption of xanthate onto pyrite is favoured in acidic conditions. In the present work, flotation tests were run at pH 7.2. The speciation diagram in Figure 7.9 has shown that under these conditions, all iron (III) will form ferric hydroxide as a stable species so that it did not affect the flotation response in the manner described above.

The work by Jiang et al. (1998) also showed that the PZC of pyrite in the presence of $2 \times 10^{-3}\text{M}$ ferrous ions is pH 9. Addition of $6.6 \times 10^{-4}\text{M}$ ethyl xanthate reduced it to pH 6. The authors observed that at $\text{pH} < 6$, the zeta potential curve was identical to that in the presence of xanthate only and at $\text{pH} > 6$, it was identical to that in the presence of only ferrous ions. From these results, they concluded that ferrous ions do not undergo significant reaction with

xanthate at pH < 6 and the flotation of pyrite in this region is mainly due to the adsorption of xanthate on the surface. At pH > 6, the adsorption of xanthate was reduced, which was in agreement with their flotation results. Similarly, the presence of ferrous ions from low pH treatment in this present work could have affected flotation recoveries by reducing xanthate adsorption. This could have been due to the formation of ferrous hydroxyl xanthate complexes in solution, rather than on the surface.

7.2.2 Uranium

The R and k values for uranium recovery are reported in Table 7.3 and the grade recovery data is presented in Figure 7.5.

Table 7.3 *Uranium final recoveries and initial rates*

Conditioning pH	k (min ⁻¹)	R _{max} (%)	R ²
1.9	0.53	21.9	0.9954
7.2	0.59	23.4	0.9947

Conditioning the plant feed at pH 7.2 prior to flotation resulted in a higher initial rate of 0.59 min⁻¹ compared to 0.53 min⁻¹ at pH 1.9 (Table 7.3). With a factor of almost 11%, the difference between the two is significant. The final recovery for pH 7.2 was also higher than that for pH 1.9 by a factor of 6.8%. Recovery-grade curves also show that pH 7.5 gave a much better flotation response throughout since its curve was always above that for pH 1.9 (Figure 7.5)

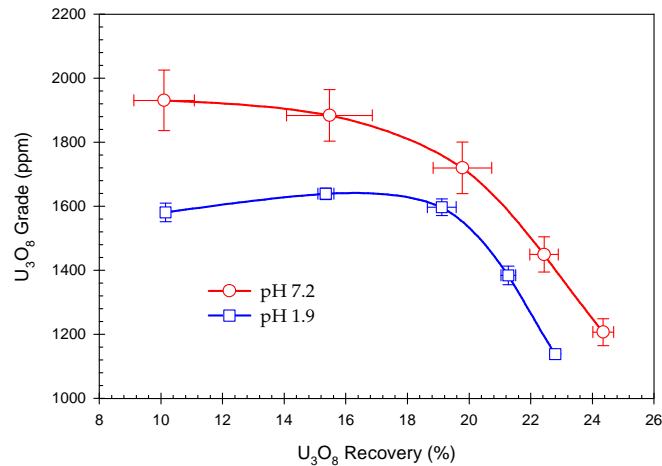


Figure 7.5 Uranium grade-recovery curves recorded following conditioning at two pH values prior to flotation.

Ores mined from the Vaal Reef contain uranium predominantly in the form of uraninite (Ford, 1993). Brannerite is also present but in much lower quantities (Brown, 2002). These are oxides, yet are floated with a sulphide collector. The effective recovery by sulphide flotation agents is probably due to the association with other minerals that respond to xanthates, or due to some activating species present on the uraninite surface.

Back-scattered Electron Imaging (BEI) and Energy Dispersive Spectroscopy (EDS) have been used to identify the minerals in concentrates recovered with SIBX. An EDS spectrum (Figure 7.7 (a)) of phase A (Figure 7.6) shows that it contains $78.95 \pm 0.83\%$ wt U as uraninite. Phase B (Figure 7.6) on the other hand contains vast amounts of sulphur and iron (Figure 7.7 (b)) as pyrite. The darkest particles (C for instance) consist of aluminosilicates, free quartz and some pyrophyllite (Figure 7.7 (c)).

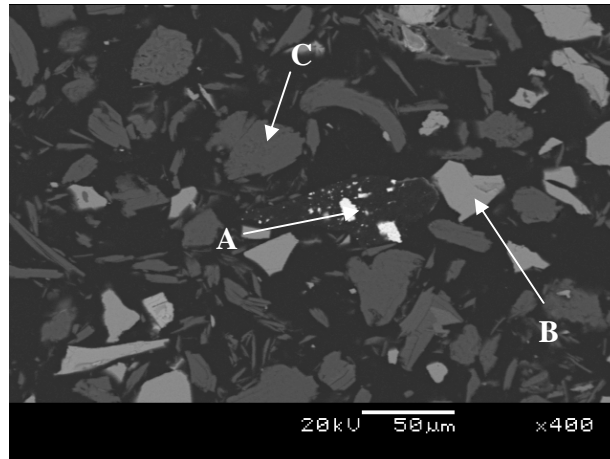


Figure 7.6 A back-scattered electron image taken from a concentrate recovered with 20g/t SIBX^{sr}

^{sr} More back-scattered images are shown in Appendix A

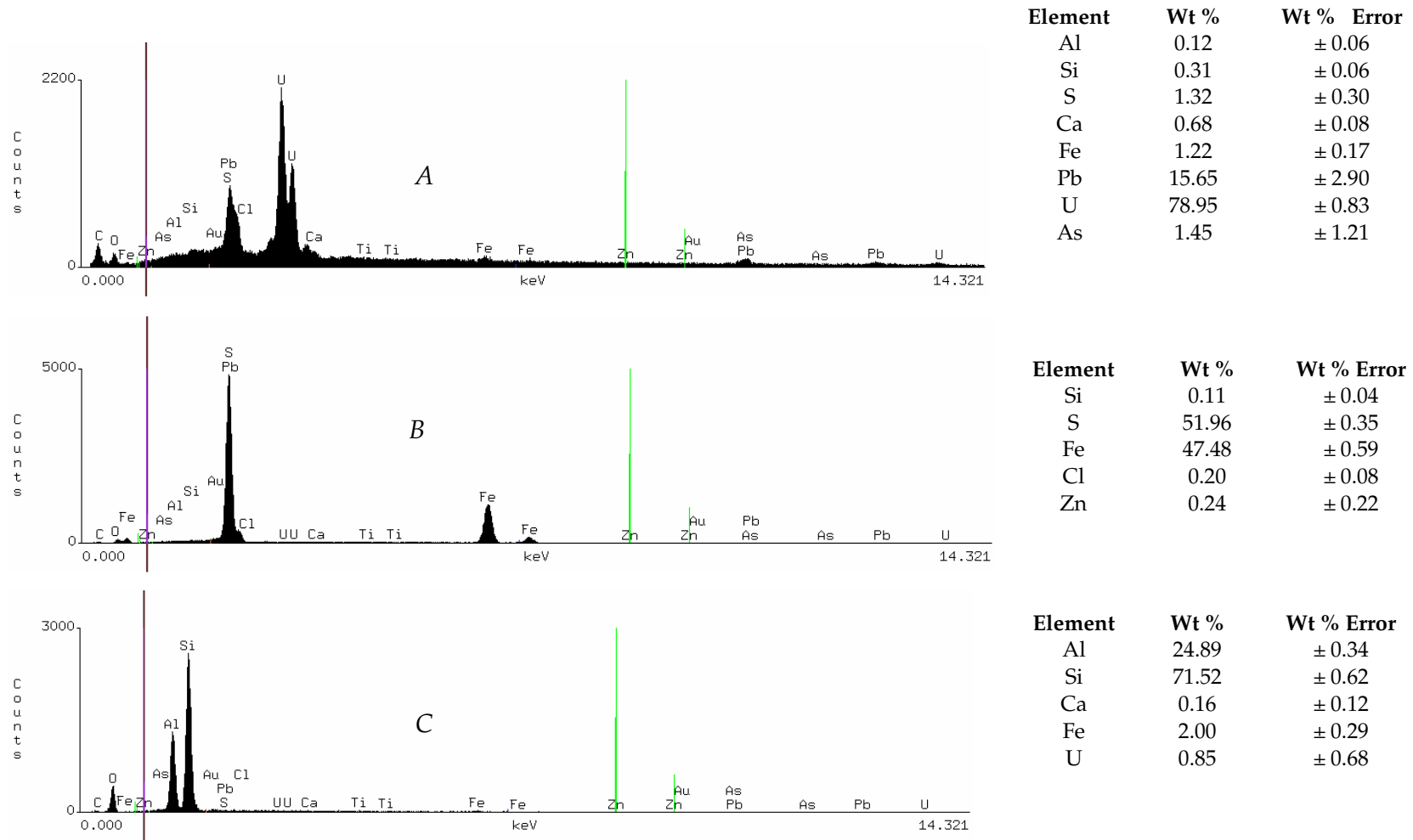


Figure 7.7 (a), (b) and (c) EDS spectra showing the elemental compositions of the corresponding phases shown in the back scattered electron image in Figure 4.32.

The presence of lead ($15.65 \pm 2.90\%$ wt) and sulphur (1.32 ± 0.30 wt %) in the EDS spectra (Figure 7.7 (a)) of phase A (Figure 7.6) suggests the presence of galena. This sulphide responds very well to flotation with xanthates (O'Dea et al., 2001; Woods, 1971; Tolun and Kitchener, 1963). Presumably the presence of lead acts as a good activator for thiol collectors.

Because of a mineralogical association between uraninite and galena, one may expect a relationship between lead and uranium recovery. Plots of lead and uranium recoveries versus mole percent of TTC dosed are shown in Figures 7.8 and 7.9. There does appear to be a relationship.

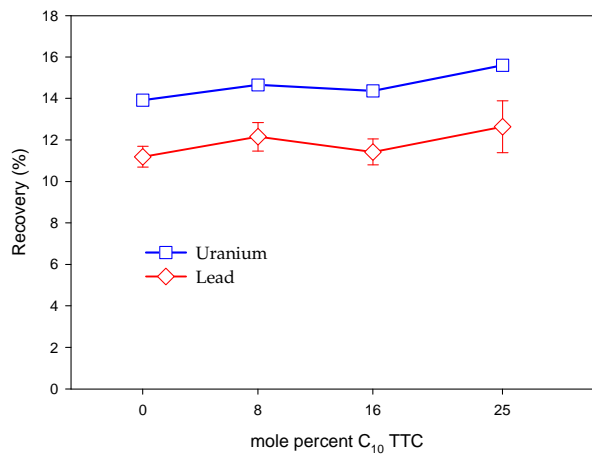


Figure 7.8 Lead and uranium recoveries for C_{10} TTC/SIBX mixtures

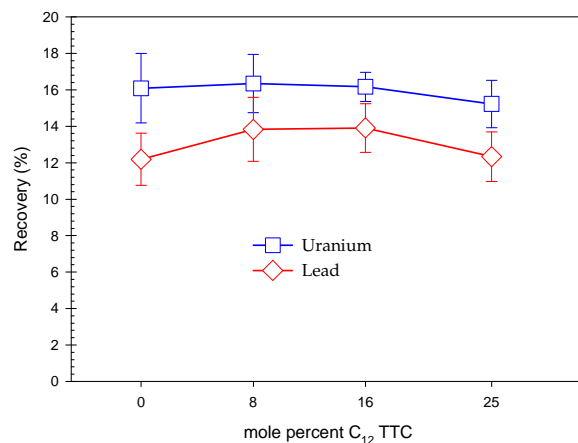


Figure 7.9 Lead and uranium recoveries for C_{12} TTC/SIBX mixtures

Particle A in Figure 7.6 shows that it is part of a dispersion of fine particles that is surrounded by a dark matrix. If the borders of the latter are traced, they compound to a particle. This is more visible in another BEI shown in Figure 7.10 below. During micro-probe analysis of a similar particle (Figure 7.11), while resin used to mount the sample was charred by the electron beam of the instrument, this matrix did not respond. This shows that the matrix differs from resin.

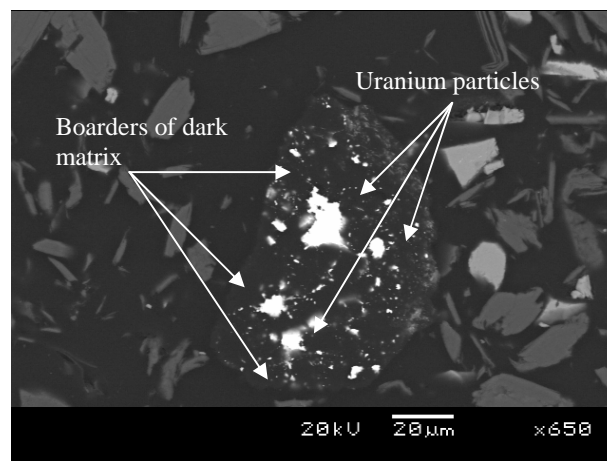


Figure 7.10 A dispersion of fine uranium-containing particles embedded in a larger particle found in a concentrate floated with 20g/t SIBX

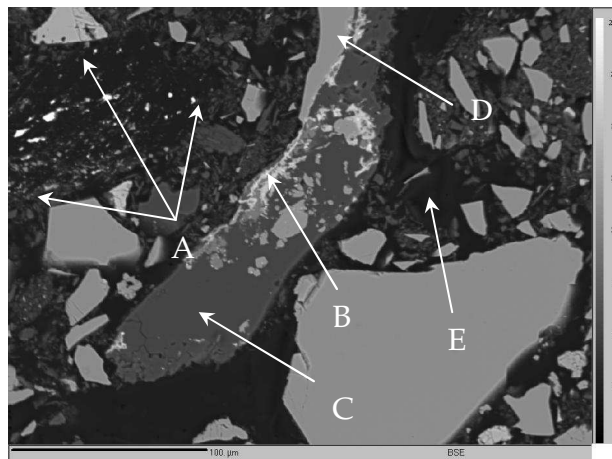


Figure 7.11 A BEI taken from the micro-probe analysis of concentrates floated with 20g/t SIBX, (A) boundaries of a dark matrix carrying a fine dispersion of uranium particles, (B) uranium particles, (C) siliceous phase, (D) pyrite and (E) charring of resin after exposure to electron beam

EDS spectra (Figure 7.13) generated from the micro-probe analysis of phase A (Figure 7.11) showed a carbon peak. Comparison between this peak³⁸ and that on spectra from an iron-sulphide (Figure 7.12) eliminates the effect of carbon introduced to increase the conductivity of the sample. Since the peak is larger, the dark matrix is carbonaceous in nature and it could be the karogen (or thucolite) that constitutes carbon seams found in the Witwatersrand Basin (Rob and Meyer, 1995; Anhaeusser et al., 1987; Simpson and Bowels, 1977). Since the carbonaceous matter is organic, it possesses natural hydrophobicity.

Another observation from the back-scattered electron image in Figure 7.11 is that uranium and pyrite co-exist in a single particle. This implies that uranium could at least partially be recovered with pyrite. The flotation behaviour following pre-flotation conditioning at pH 1.9 can be accounted for through the mineralogical relationships with pyrite, karogen and galena.

³⁸ Note that the peak labelled [O] in Figure 4.39 is actually a carbon peak

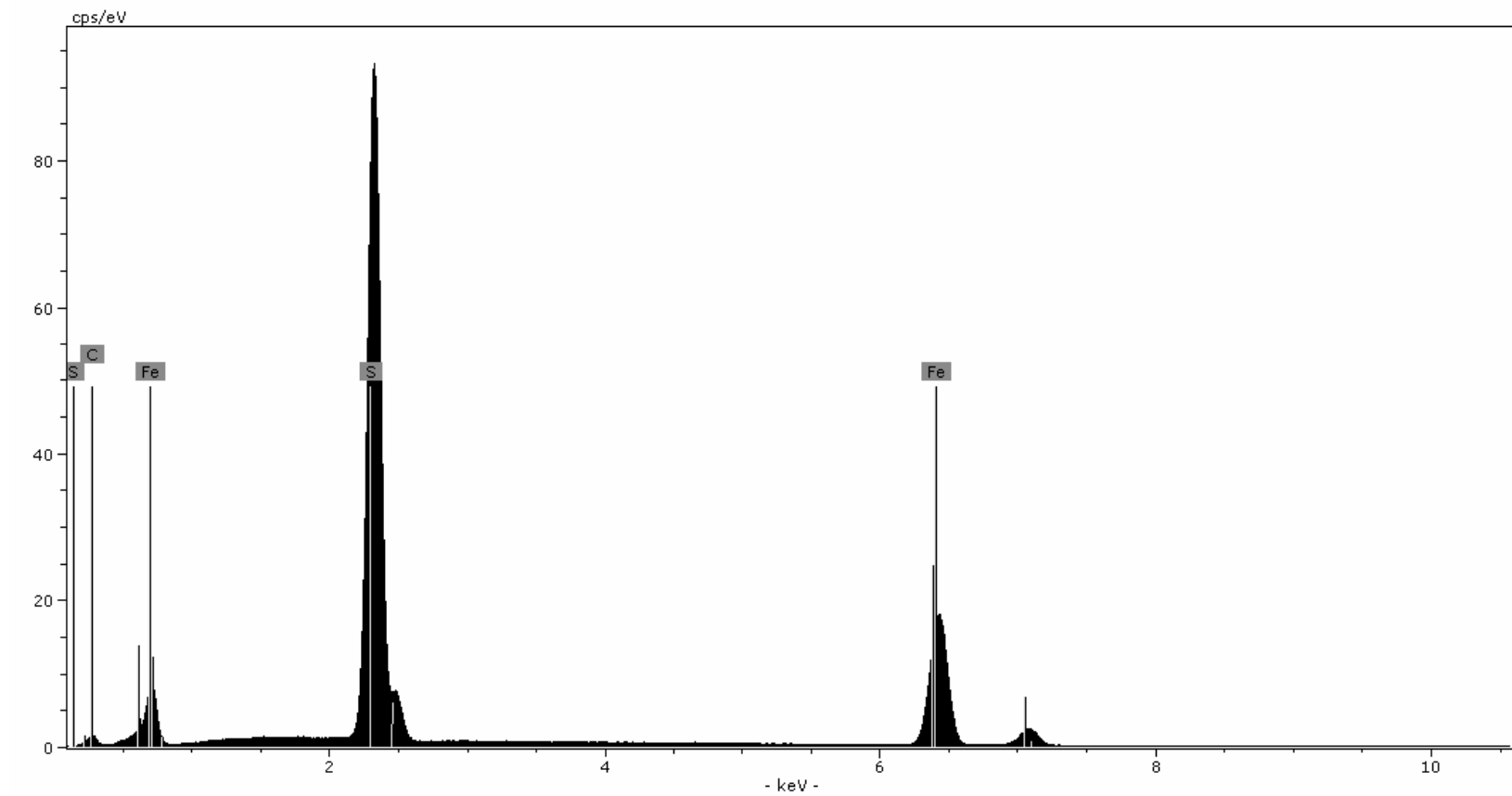


Figure 7.12 EDS spectra generated from the microprobe analysis of an iron sulphide

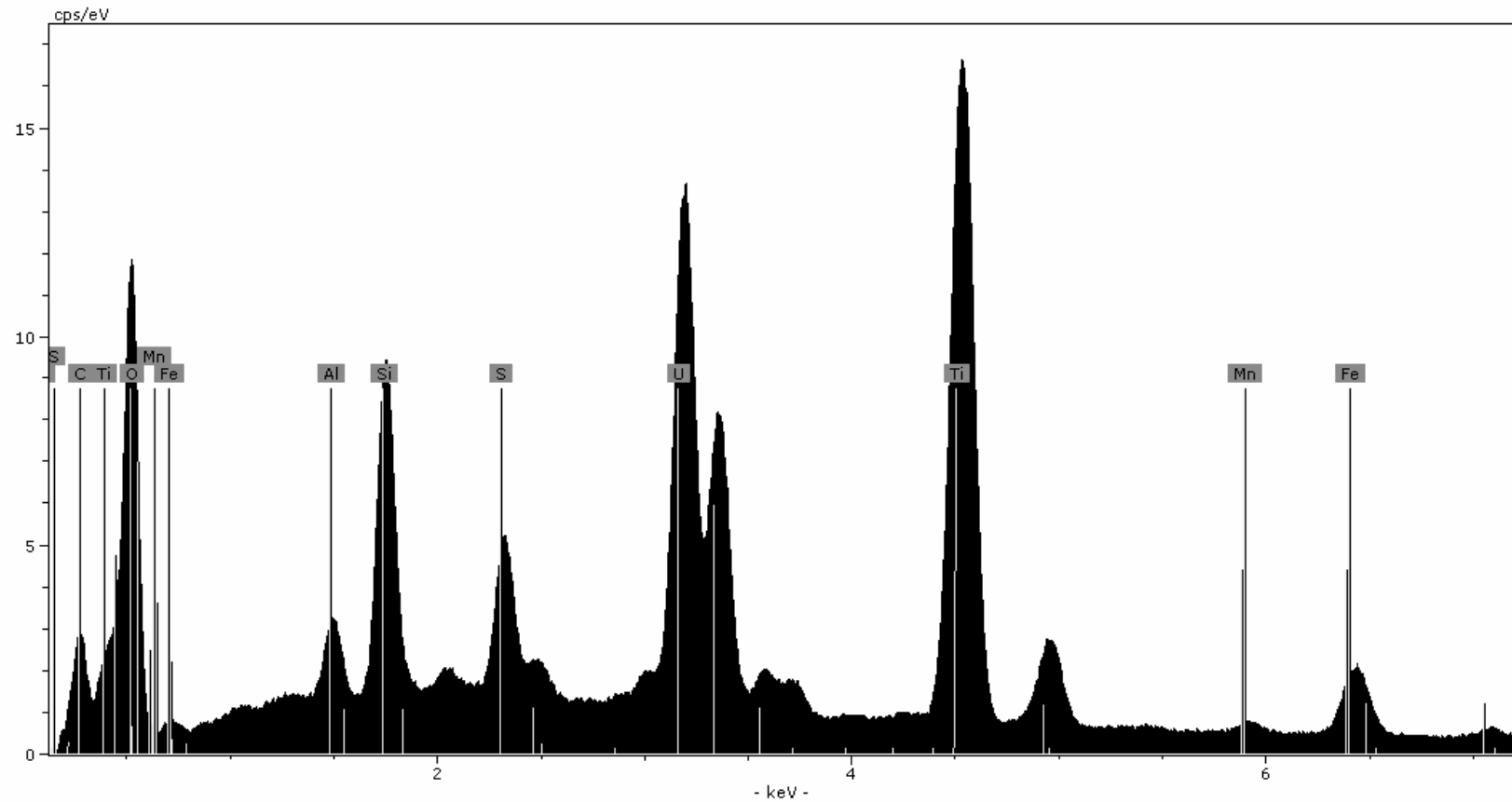
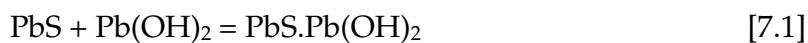


Figure 7.13 EDS spectra generated from the microprobe analysis of the dark phase found in a concentrate recovered with 20g/t SIBX.

Karogen is not expected to undergo chemical change at low pH because it is essentially carbon. It might however adsorb ferric hydroxide, ferrous ions and the respective hydroxyl complexes. Interaction between xanthate and the adsorbed species will form hydroxyl xanthate complexes, which will enhance flotation of karogen. This would consequently improve flotation of the hosted uranium.

The flotation response of galena can be predicted by using thermodynamic data to establish the species formed on the surface. Figure 7.13 shows a Pourbaix diagram for the Pb-S-H₂O system in which E_h-pH conditions encountered in each conditioning stage (Table 7.2) have been superimposed. Natural pulp potential and pH (point A) fall in the domain of Pb(OH)₂ stability so that galena is likely to be coated by lead hydroxide. Conditions prevailing immediately after acid addition and 10 minutes of conditioning (points B and C) both predict the formation of PbSO₄. After addition of a caustic solution to adjust pH to the standard flotation pH, Pb(OH)₂ is formed. This implies that the flotation behaviour of galena is controlled by interactions between lead hydroxide and the collector. O'Dea and co-workers (2001) have proposed a mechanism in which the hydroxide attaches to the surface of galena (equation 7.1). An exchange reaction between xanthate and hydroxide may then take place (equation 7.2). Oxidation of xanthate to dixanthogen accompanied by oxygen reduction may follow (equation 4.3).



In this way, a mineralogical association between galena and uranium minerals should enhance recoveries after low pH conditioning.

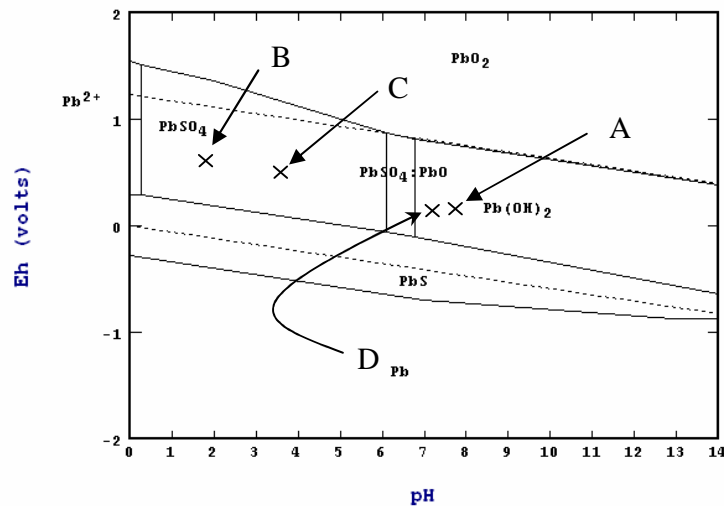


Figure 7.13 A Pourbaix diagram for the Pb-S-H₂O system at 25°C, 10⁻³M [Pb], 10⁻³M [S] showing E_h-pH conditions prevailing during conditioning [A] natural pulp E_h-pH, [B] soon after addition of 1.25kg/t sulphuric acid, [C] after 10 minutes of conditioning, [D] after addition of a caustic solution to attain standard flotation pH

4.4.3 Gold

Table 7.4 shows gold final recoveries and initial rates for the two conditioning pHs tested. Corresponding recovery-grade curves are shown in Figure 7.14. The curve for pH 1.9 is above that for pH 7.2 throughout, which implies a better flotation response. This is also evidenced by their flotation initial rates; pH 1.9 recorded 0.65min⁻¹ while the latter gave 0.53min⁻¹. A similar trend was observed in the final recoveries, 43.9% compared to 41.5 %.

Table 7.4 Gold final recoveries and initial rates

Conditioning pH	k (min ⁻¹)	R _{max} (%)	R ²
1.9	0.65	43.9	0.9931
7.2	0.53	41.5	0.9956

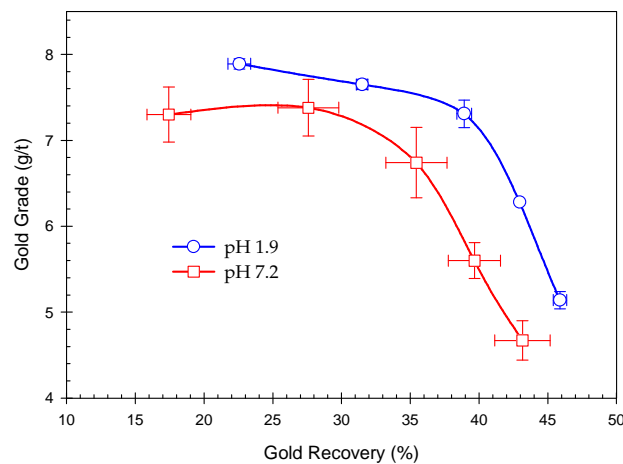


Figure 7.14 Gold recovery–grade curves plotted from data recorded from experiments in which No 2 Gold Plant feed was conditioned at pH 1.9 and pH 7.5 prior to flotation

Since gold is associated with cyanide insoluble pyrite (Parnell, 2001; Rob and Meyer, 1995; Ford, 1993), recovery of this sulphide accounts for the recovery of gold from leach residues (de Wet et al., 1995). Part of the feed to the plant consists of reclaimed old dump material so that the sulphide is likely to be oxidised. This is further influenced by air that is introduced to meet the oxygen requirement of the cyanidation process. Low pH treatment prior to flotation has already been shown to result in higher kinetics and lower final recoveries. Rob and Meyer (1995) have also mentioned the presence of gold in quartz veins in the Witwatersrand basin. This fraction, if partially liberated will not be fully soluble in cyanide. Acid conditioning could have polished the gold, and improved interaction with flotation reagents.

7.2.4 Conclusions

Based on release curve experiments, conditioning at pH 1.9 gave significantly higher sulphur flotation kinetics and slightly lower final recoveries compared to the standard pH of 7.2. Uranium initial rates were higher although recovery-grade curves showed that the standard pH was better all through. In fact, uranium lost flotability considerably because the curve for the standard was above throughout. Gold initial rates and final recoveries were significantly improved by the low pH treatment. This was also shown in the corresponding recovery-grade curve that was above the standard throughout.

Through use of EDS analysis and back-scattered electron images from microprobe analysis and scanning electron microscopy, all uranium-bearing particles recovered with SIBX were shown to have an association with pyrite, galena and/or karogen. The flotation of uranium was therefore attributed to these relationships since all these minerals are floatable.